Supporting Information

Focused Ultrasound Propulsion of Acoustically Active Nanoparticles into Gelatin Hydrogels

Talaial B. Alina,[a] Shane D. Curry,[a] Sven A. Saemundsson,[a] Bryce M. Bower,[a] Jennifer N. Cha,[a,b,c,] Andrew P. Goodwin[a,b,*]*

[a]Department of Chemical and Biological Engineering, [b]Materials Science and Engineering Program, and [c]Biomedical Engineering Program, University of Colorado Boulder, Boulder, Colorado 80303, United States.

*jennifer.cha@colorado.edu, *andrew.goodwin@colorado.edu

MATERIALS AND METHODS:

1. General Materials.

Glass scintillation vials (4 mL) were purchased from DWK Life Sciences Kimble, and NMR tubes were obtained from Wilmad-LabGlass. Chemicals acquired from Sigma-Aldrich included dichloromethane (anhydrous, ≥ 99.8%), gelatin from porcine skin (Type A, gel strength ~300), and tetraethylorthosilicate (TEOS, ≥ 99%, GC). NHS-rhodamine, triethanolamine (TEA, 98+%), and 96-well plates were obtained from Thermo Scientific. Octadecyltrichlorosilane (ODTS, 97%) was purchased from Acros Organics, and polyethylene glycol 2000 (PEG 2000) from TCI America. Anhydrous 200 proof ethanol was obtained from Decon Laboratories. Ultrapure (UP) water (HPLC grade), hydrochloric acid (Certified ACS Plus, 36.5–38.0% w/w), and 20 mL glass scintillation vials were purchased from Fisher Chemical and Fisher Scientific. Glass slides (25 × 75 × 1 mm), glass coverslips, and 50 mL tubes were purchased from VWR. BD Luer-Lock syringes (diameter: 26.6 mm) and BD PrecisionGlide needles (0.6 mm × 25 mm) were obtained from BD. Lipids including 1,2-dibehenoyl-sn-glycero-3-phosphocholine (DBPC) and 1,2-distearoyl-sn-glycero-3-phosphoethanolamine-N-[methoxy(polyethylene glycol)-2000] (DSPE-PEG2K-methoxy) were purchased from Avanti Polar Lipids. 3 mL transfer pipettes were obtained from Corning Falcon. Petri dishes (15 × 100 mm) were purchased from TWD Scientific. A ToteAll 2000 container (25 × 15.5 × 8.75 in.) used for ultrasound insonation studies in water was purchased from United States Plastic Corp.

2. Synthesis of mesoporous silica nanoparticles (MSNs).

Mesoporous silica nanoparticles (MSNs) were synthesized using a modified version of our previously reported protocol.[1] To prepare the fluorescent tag, 3.3 mg NHS-Rhodamine was combined with 1 mL of the extracted anhydrous DMF and 12.22 µL (3-aminopropyl)triethoxysilane (APTES) in a 4 mL scintillation vial. The solution was then purged with argon, sealed with Parafilm, and shaken in the dark for 24 h.

The synthesis began by combining 5 mL of cetrimonium chloride (CTAC) with 15 mL ultrapure water in a 50 mL round-bottom flask equipped with a medium-sized egg stir bar and a condenser. The mixture was heated to 75°C and stirred at 380 RPM. A 10% v/v triethanolamine (TEA) solution was prepared by mixing 90 µL TEA with 810 µL ultrapure water, and 800 µL of this solution was added to the reaction vessel. After heating at 80°C for 45 min, 1.5 mL tetraethyl orthosilicate (TEOS) was introduced in three sequential 500 µL additions over 1 min, and 500 µL of the APTES–NHS-Rhodamine conjugate was added in five sequential 100 µL additions over 1 min. The reaction was maintained at 80°C with continuous stirring for 90 min.

The product was transferred to 50 mL conical tubes, and the reaction vessel was rinsed with anhydrous ethanol to ensure complete transfer. Particles were collected by centrifugation at 7100 RCF for 30 min and washed twice with 15 mL of anhydrous ethanol.

CTAC template removal was performed through three cycles of acidic ethanol treatment. In each cycle, particles were dispersed in a solution of 375 µL of 37% hydrochloric acid (HCl) and 30 mL ethanol, then heated at 65°C with stirring at 660 RPM for 2 h. Afterwards, the particles were collected by centrifugation at 7100 RCF for 30 min. Following template removal, the particles were washed twice more with ethanol and transferred to a 20 mL scintillation vial. The final product was obtained by evaporating the ethanol to the atmosphere in an open vial at 65°C overnight.

3. Synthesis of hydrophobically modified mesoporous silica nanoparticles (HMSNs).

The hydrophobic modification of MSNs was performed following a modification of our previous work.[2] A suspension was prepared by combining 55 mg MSNs with 10 mL anhydrous dichloromethane in a 50 mL round-bottom flask. After 5 min of sonication, the headspace was purged with argon for 30 s before slowly adding 300 µL octadecyltrichlorosilane. The mixture underwent an additional 5 min of sonication followed by a 30-second argon purge. Then, the reaction vessel was sealed with a glass stopper and Parafilm, and stirred with a medium-sized egg stir bar at 700 RPM at room temperature for 24 h.

The product was collected by dividing the suspension between two 50 mL conical tubes, using hexane to rinse the reaction vessel and ensure complete transfer. Particles were isolated by centrifugation at 7100 RCF for 30 min. They were then purified by two washes with 30 mL hexane followed by one wash with 30 mL anhydrous ethanol, using the same centrifugation conditions for each step. The purified HMSNs were dispersed in 20 mL anhydrous ethanol, transferred to a 20 mL glass scintillation vial, and dried at 65°C in an oil bath overnight with exposure to air.

4. Synthesis of phospholipid coated, hydrophobically modified silica nanoparticles (PL-HMSNs).

The synthesis of phospholipid-coated, hydrophobically modified mesoporous silica nanoparticles (PL-HMSNs) was adapted from our previous work.[2] Stock solutions were prepared by dissolving lipids in 10 mg mL^{-1} chloroform and HMSNs in 5 mg mL^{-1} chloroform, followed by 30 s of sonication. The coating mixture was prepared at a ratio of 2.725 µmol lipid: 0.214 µmol pegylated lipid: 4 mg HMSNs. This was achieved by combining 246 µL of 10 mg mL^{-1} 1,2-

dibehenoyl-sn-glycero-3-phosphocholine (DBPC), 60 µL of 10 mg mL^{-1} 1,2-distearoyl-sn-glycero-3-phosphoethanolamine-N-[methoxy(polyethylene glycol)-2000] (DSPE-PEG2K-methoxy), and 800 µL of 5 mg mL^{-1} HMSN suspension.

The coating process began by heating ultrapure water under stirring at 1000 RPM and 50°C in a 20 mL vial for 15 min with two small egg stir bars. The coating mixture was then added. The preparation vessel was subsequently rinsed twice with 1000 µL of chloroform, with the final rinse being sonicated for 15 seconds before addition to the main reaction. The combined mixture was maintained at 79°C with continuous stirring at 1000 RPM for 3 h to remove chloroform by evaporation.

Following overnight aging at 4°C, the product was transferred to 1.5 mL tubes, with the reaction vessel rinsed with three 1 mL portions of ultrapure water to ensure complete transfer. The particles were consolidated by centrifugation at 2500 RCF for 10 min and purified through three additional centrifugation–wash cycles using 1 mL ultrapure water per wash.

5. Diffuse reflectance infrared Fourier transform spectroscopy (DRIFTS).

The protocol for performing Diffuse reflectance infrared Fourier transform spectroscopy (DRIFTS) was adapted from a paper by Alina et al. (2024).[2]

DRIFTS characterization identified the functional groups of MSNs and DBPC HMSNs. The process involved adding about 100 mg of samples in dried powder form. A Thermo Fisher Scientific Nicolet 6700 FTIR performed the analysis. Python was used to perform baseline subtraction and generate relevant stacked plots where data was normalized to the peak across the 3500 cm^{-1} and 700 cm^{-1} range.

6. Dynamic light scattering (DLS) and zeta potential measurements.

The protocol for performing dynamic light scattering (DLS) and zeta potential measurements was adapted from a paper by Alina et al. (2024).[2]

Dynamic light scattering (DLS) measurements of MSNs and DBPC HMSNs in 1× PBS were performed in triplicate using an Anton Paar Litesizer 500 at 25 °C under automatic run conditions with the detection angle set to backscatter. Zeta potential measurements used 1 mg mL^{-1} samples in 1X PBS and an Omega cuvette Mat. No. 225288. The instrument's default analysis (Smoluchowski approximation in aqueous electrolyte) was used unless otherwise noted. For Python plotting, replicate distributions were interpolated to a common diameter grid and averaged; the mean curve is shown with a shaded band indicating ±1 standard deviation of mean across replicates. Axes were truncated beyond regions contributing <0.1% of the total distribution to enhance visual clarity without affecting the reported size statistics.

7. Fabrication of hydrogel transport system.

The protocol for fabricating gelatin hydrogels was adapted from Alina et al. (2020).[3] First, 10X phosphate-buffered saline (PBS) was diluted to 1X using deionized (DI) water. To degas the 1X PBS, 1 L of the solution was subjected to four degassing cycles. In each cycle, the solution was first brought to a boil, then stirred at 350 RPM under full house vacuum for 5 min using a long rod stir bar in a 1 L reaction beaker, followed by 5 min of light stirring at 350 RPM under an argon atmosphere using needle-based argon sparging. After completing all four cycles, the degassed solution was stored at room temperature under an argon blanket and sealed with Parafilm.

A 17% (w/v) gelatin stock solution was prepared by dissolving dry gelatin in degassed 1X PBS that had been boiled and subsequently cooled to 45°C prior to gelatin addition. The mixture was stirred at 600 RPM for 1 hour until fully dissolved. To prepare 2%, 4%, and 8% (w/v) working

solutions, the stock was diluted with degassed 1X PBS and 1% (w/v) sodium azide (also prepared in degassed 1X PBS). Sodium azide served as the bacteriostatic agent, yielding a final concentration of 0.1% (w/v). All solutions were mixed at 45°C in 250 mL reaction flasks using a medium-sized egg stir bar at 600 RPM until homogeneous. Stirring was slowed down afterwards to prevent excessive bubble formation.

To create cylindrical molds, the narrow junction between the bulb and stem of 3 mL Falcon transfer pipettes was cut, and the stem was inverted so that its open end faced upward to hold the gel. To seal the gap between the tip of the inverted transfer pipette stem and the interior of the severed bulb, 1 mL of gelatin solution, pre-warmed to 45°C, was pipetted into the center of each mold and allowed to gel at room temperature for 2 h. . The molds were covered with Parafilm to prevent dust ingress. This sealing step ensured no leakage during subsequent additions. Next, due to limited hot plate availability, each gelation solution prepared initially was individually heated to 45°C prior to the second addition of gelatin. Afterwards, an additional 1 mL of the same solution was added to fill the mold and form the full cylindrical hydrogel. The assembled gels were left to set overnight at room temperature and covered with Parafilm and aluminum foil to minimize evaporation.

8. Preparation of ultrapure water and PEG 2000 solutions.

The weight fraction of PEG 2000 required to achieve specified solution viscosities was determined by inverting the empirical correlation of Murugesan and Perumalsamy, who measured viscosities of aqueous PEG 2000 at 5–50 wt% and provided the cubic nonlinear fit (Equation S1)

Equation S1 $$\eta(w) = 447.5w^3 - 114.25w^2 + 20.847w + 0.894$$

(where η is the dynamic viscosity in mPa·s and w is mass fraction).[4]

To obtain the mass fraction corresponding to target viscosities of 1, 5, and 10 cP, Equation S2

Equation S2 $$\eta(w) - \eta_{target} = 0$$

was solved numerically using NumPy's roots routine, which computes the eigenvalues of the companion matrix to yield all polynomial roots.[5] Of the three roots returned for each target, the physically meaningful real root in the interval [0,1] was selected and multiplied by 100 to express the result as weight percent (wt%) of PEG 2000 in the solution. At room temperature, approximated as 25°C, the PEG 2000 mass fractions required to reach dynamic viscosities of 5 cP and 20 cP are 22.8 wt% and 40.3 wt%, respectively (assuming the base ultrapure water viscosity is ~1 cP).

9. Ultrasound characterization of particles by passive cavitation detection.

The high intensity focused ultrasound (HIFU) setup was adapted from a protocol by Alina et al. (2023).[6]

Prior to the experiment, the water bath was thoroughly cleaned with soap and deionized (DI) water, then filled to a height of 4.5" with DI water.

A waveform generator (Agilent Technologies 33522A) was connected to a power amplifier (T&C Power Conversion AG1020) and set to the following parameters: frequency = 1.1 MHz, waveform = sine wave, amplitude = 1 Vpp, burst period = 1 ms (1 kHz), output from channel 1. The amplifier operated at 100% output with a gain of 55 ± 1.5 dB and was connected to an

impedance-matching network (Sonic Concepts, S/N 119), which drove the 1.1 MHz transducer (Sonic Concepts H-101; 64.0 mm active diameter, 63.2 mm radius of curvature).

The transducer was mounted inside a coupling cone, and the total height of the assembly was 63 mm.[7] The setup was kept fully submerged to ensure the cone remained filled with deionized (DI) water. According to the manufacturer, the focal volume of the transducer is approximately 15 µL (1.37 mm diameter × 10.21 mm length). The transducer converted electrical signals into focused acoustic energy directed at the sample. The sample—typically a 200 µg/mL particle solution or a blank control—was dispensed using a 1 mL pipette into a transfer pipette whose tip had been trimmed with scissors to widen the opening. Only the 4 mg/mL MSN stock solutions were sonicated to disperse particles prior to their dilution and addition to the transfer pipette to avoid disrupting the lipid coating on DBPC HMSNs.

A 20 MHz immersion transducer (Olympus Panametrics V317), placed orthogonally and in contact with the sample holder, captured the acoustic emissions from cavitation events. These signals were amplified 40 dB using a pulser/receiver (Olympus 5072PR) with the following settings: pulse repetition frequency = 100, energy level = 1, damping = 3 (50 ohms). The signal was then passed through a 6.7 MHz high-pass filter (Thorlabs EF513) and displayed on an oscilloscope (Tektronix TBS1000), which averaged every 64 data points with vertical and horizontal scales set to 200 mV/div and 25 µs/div, respectively. The external trigger level was set to –168 mV.

The number of cycles on the waveform generator was varied from 0 to 110, corresponding to duty cycles ranging from 0% to 10%. The specific cycle counts and their corresponding duty cycles were as follows: 0 cycles (0%), 1 cycle (0.1%), 5 cycles (0.5%), 11 cycles (1%), 28 cycles (2.5%), 40 cycles (3.6%), 55 cycles (5%), and 110 cycles (10%). Samples were typically insonated for 10 seconds. Oscilloscope output data were exported as .CSV files. After saving the data as a .CSV file, a custom MATLAB program was developed to compute the pulse-averaged signal intensities.[8] Voltage signals from 35–60 µs were squared and integrated using the trapezoidal method. The resulting values were then normalized to the signal intensity measured in the absence of ultrasound (Equation S3).[9] For PEG2000 solutions, the mean cavitation threshold was defined as the lowest duty cycle at which the pulsed signal intensity exceeded the mean plus three standard deviations of the 0% duty cycle signal.

Equation S3

$$I_{norm} = \frac{\int_{35\,\mu s}^{60\,\mu s} mV^2(t) * dt}{I_0}$$

10. Ultrasound insonation of pipette-bulb system

Prior to transport studies, 1 mL of 1X PBS, previously degassed and equilibrated in a closed container, was added to the prepared PL-HMSN pellets to achieve a final concentration of 4 mg mL^{-1}. An aliquot was then extracted and combined with 1X PBS to form a 200 µg mL^{-1} particle solution. PL-HMSNs were readily dispersed by pipetting. Separately, dried MSNs were dispersed in 1X PBS to a final concentration of 200 µg mL^{-1} using brief sonication to ensure uniform suspension. Following the setup described in Section 9, 200 µL of the 200 µg mL^{-1} particle solution was added to an empty pipette bulb with its stem cut off. For studies investigating the effect of particle concentration on total penetration area, 25 µg mL^{-1} and 200 µg mL^{-1} MSN and DBPC-HMSN solutions were individually prepared from stock suspensions.

The pipette bulb was secured upright using clamps and positioned directly on top of the coupling cone housing a 1.1 MHz transducer. The total height of the transducer and coupling cone assembly was 63 mm.[7] To minimize acoustic scattering from air interfaces, the bulb and cone assembly was fully submerged in deionized (DI) water such that approximately half of the bulb's exterior was covered. This ensured that the cone remained filled and in acoustic contact with the water.

The gelatin-containing pipette, prepared with the wide bulb facing up and the narrow tip down as described in Section 7, was sliced at the gel meniscus at the wide bulb end using a razor. The pipette was then returned to its upright orientation and briefly shaken in a large bath of deionized water to remove residual gelatin from cutting. Then, the pipette was gently blotted on a paper towel to remove residual water. Finally, the cleaned pipette was placed on top of the particle-filled bulb, forming a sealed interface. The combined assembly was clamped in place to maintain alignment.

High-intensity focused ultrasound (HIFU) was applied using the parameters described in Section 9, with a treatment time of 1 minute. The number of cycles—and the corresponding duty cycles—varied by condition: 0 cycles (0%), 1 cycle (0.1%), 5 cycles (0.5%), 11 cycles (1%), 28 cycles (2.5%), and 40 cycles (3.6%). For 2% and 4% gelatin, cycles varied from 0 to 28. For 8% gelatin, the 40 cycle condition was also included.

For studies monitoring temperature changes in the feed solution before and after HIFU exposure, a fiber optic temperature probe connected to a J-Kem Scientific Model 210 controller was positioned in the feed solution adjacent to the gelatin–solution interface, within the region outside the gel. The probe was equilibrated for several seconds before recording the initial temperature. Immediately following HIFU treatment, the gelatin mold was removed and the probe was repositioned to the center of the bulb to measure the post-treatment temperature. The temperature change (ΔT) was calculated as the difference between post- and pre-HIFU measurements. For control (no HIFU) conditions, the probe remained immersed in the feed solution for 1 minute.

11. Hydrogel confocal microscopy imaging

After HIFU insonation, each inverted pipette mold containing a hydrogel was placed onto a flat board with a hole that securely held the pipette bulb in place. The pipette was held steady by hand throughout cutting. A longitudinal cut was initiated at the thickened junction near the center of the pipette—typically where the cylindrical stem meets the rounded bulb—and guided smoothly along the edge of the hydrogel cylinder using a razor blade. Once the blade reached the narrow tip at the bottom of the pipette, a gentle back-and-forth motion was used to complete the cut through the smaller diameter section. This method ensured clean sectioning and consistent imaging surfaces while preserving gel integrity. Sliced gels were then placed into 100 × 15 mm petri dishes.

Immediately prior to imaging, triplicate gels were sliced with scissors ~2 cm from the wider bulb end of the inverted mold, yielding six sections for imaging, which were stored in a petri dish. Groups of six transverse gel sections were then placed on 25 mm × 75 mm × 1 mm glass slides pre-cleaned with deionized water and a lint-free wipe. A sucrose solution prepared in ultrapure water was then added dropwise using a transfer pipette to match the refractive index of each gel: 2.5% (w/v) for 2% gelatin, 5% for 4% gelatin, and 10% for 8% gelatin.[10,11] Any air bubbles introduced during addition were gently removed by vertically displacing the gel up and down against the slide surface. Brightfield microscopy was first used to locate the bottom leftmost gel section. Imaging was then performed sequentially from left to right gel sections. Fluorescence imaging was carried out using a 561 nm excitation laser with a pinhole size of 3 Airy units, scanning speed set to 1

(slowest/highest-quality), 20-frame averaging, and a pixel dwell time of 2.5 µs. Channels were acquired in Sequential Galvano mode using Galvano scanning, and each gel was imaged using a 3 × 9 tile-stitch configuration. A 256 × 256 pixel field of view was initially used to localize the gel interface (see screenshot, bottom right), while stitched images were acquired at 1024 × 1024 resolution. Z-stack images were collected with a step size of 1.55 µm, covering a total imaging depth of 80 µm.

12. Parallel plate rheology testing.

Rheological measurements were conducted using an ARES G2 rheometer (TA Instruments, serial number 4010-0778) equipped with a temperature-controlled environment maintained at 25°C. Hydrogel samples, prepared as described in Section 7, were subjected to high-intensity focused ultrasound (HIFU) treatment. Immediately following HIFU exposure, cylindrical hydrogel molds were sectioned to obtain 4 mm-thick discs from the bottom using a razor blade. For studies investigating how storage modulus varied with distance from the bottom surface of the hydrogel where HIFU was applied, gels were sectioned into bottom (0–4 mm) and top (4–8 mm) layers prior to measurement. A spatula was inserted along the edges between the plastic mold and the hydrogel disc to loosen the interface, and the hydrogel was then carefully scooped out. These discs were placed between parallel plates of the rheometer, ensuring consistent geometry and contact. Frequency sweep tests were performed over an angular frequency range of 0.1–100 rad/s at a constant strain amplitude of 1%, with data points logarithmically spaced at ten points per decade. The rheometer recorded oscillatory stress, storage modulus (G'), loss modulus (G''), loss tangent ($\tan\delta$), and complex viscosity (η^*) as functions of angular frequency. Rheological measurements were performed on three independently treated hydrogel samples, with each tested separately and the geometry cleaned between runs.

13. TNBS (2,4,6-trinitrobenzenesulfonic acid) assay.

Hydrogels were treated as described in Section 10. After treatment, approximately 150 µL of feed solution was collected. To each 1.5 mL microcentrifuge tube, 150 µL of feed solution, 350 µL of triethanolamine buffer (pH 8.5), and 500 µL of 0.1% (w/v) 2,4,6-trinitrobenzene sulfonic acid (TNBSA; diluted from a 5% (w/v) stock in water) were added. The mixture was combined using reverse pipetting and incubated at 37°C for 2 h. Following incubation, 250 µL of 10% sodium dodecyl sulfate (SDS) and 125 µL of 1 N HCl (diluted from an 11.65 N stock) were added and mixed again by reverse pipetting. Finally, 200 µL of each reaction mixture was transferred to a clear 96-well plate, and absorbance was measured at 335 nm.

14. Hydrogel scanning electron microscopy.

Hydrogels subjected to HIFU treatment were prepared for scanning electron microscopy (SEM) using a Hitachi TM-4000Plus II tabletop SEM equipped with energy-dispersive X-ray spectroscopy (EDS). Following treatment, a ~1 mm-thick section was excised from the bottom of each hydrogel using a razor blade. Samples were flash-frozen in liquid nitrogen and lyophilized overnight. The dried gels were mounted on conductive aluminum tape affixed to SEM stubs.

SEM imaging was performed in backscattered electron (BSE) mode at an accelerating voltage of 10 kV. Images were acquired at a resolution of 2560 × 1920 pixels using *Capture_Slow* scan speed and processed in grayscale.

Pore analysis was performed using custom Python scripts employing PoreSpy and scikit-image libraries. For each SEM image, a region of interest was manually selected and the pixel-to-

micrometer scale was automatically extracted from the TM-4000Plus metadata. Images can be binarized using various thresholding methods (Otsu, Li, Multi-Otsu, adaptive, and percentile-based) with interactive manual adjustment via a slider interface to optimize pore detection. Individual pores were segmented using the SNOW (Sub-Network of an Oversegmented Watershed) algorithm to prevent merging of adjacent pores. Morphological parameters including equivalent diameter, area, perimeter, eccentricity, and solidity were calculated for each detected pore. Porosity was determined as the ratio of pore pixels to total pixels within the ROI. Size distributions were analyzed using both number-based and volume-weighted approaches. All measurements were exported to Excel files containing summary statistics, individual pore data, and distribution parameters. The analysis code has been made available in a GitHub repository.[7]

15. Hydrogel transport investigation tutorial.

Quantitative analysis of hydrogel images was performed using a custom-built, semi-automated workflow developed in Python (v3.11).[7] This workflow integrates several key libraries, including OpenCV for core image processing tasks, ipywidgets and Plotly for creating interactive user interfaces, and pandas and numpy for robust data manipulation and analysis. The entire process guides the user through a sequential pipeline of file selection, image pre-processing, region of interest (ROI) definition, and quantitative analysis, culminating in the automated generation of detailed data reports and publication-quality figures.

Analysis began with stitching six individual ND2 images collected from imaging triplicate treatments. These were processed using a custom Python script that automatically loaded supported image files from a selected folder, extracted the physical scale (μm/pixel) using embedded metadata (OME-XML, voxel size, or TIFF resolution tags), and stitched them side by side into a single composite image. The resulting TIFF file preserved exact scale information through standardized resolution tags and OME metadata, ensuring consistent and accurate physical measurements in subsequent analysis.

In a separate Jupyter notebook, the user then selected either a single TIFF file (e.g., .tif, .tiff, or .ome.tiff) or a directory containing multiple TIFF images, typically including the stitched output. The workflow automatically loaded the selected image and determined the physical scale by parsing OME-XML metadata, TIFF resolution tags, or ImageJ headers. This scale factor was used for all downstream physical measurements..Following image loading, an interactive pre-processing interface was presented to the user. This interface allowed for several critical adjustments on a downsampled version of the image to enhance feature visibility and correct for common microscopy artifacts. These adjustments included: (i) manual optimization of brightness and contrast via Min Intensity and Max Intensity sliders; (ii) pseudo flat-field correction using a user-defined Flat-field kernel to normalize non-uniform illumination; and (iii) optional removal of high-intensity "dust" artifacts using an adaptive thresholding algorithm with adjustable Block size, Sensitivity, and Max dust size parameters.

After pre-processing, the user specified the number of experimental replicates present in the image. For each replicate, an interactive window was launched to define the ROI by drawing a rotatable and resizable rectangle. This enabled the precise selection of replicates that were not necessarily aligned with the image axes. Subsequently, each ROI was processed individually to standardize its orientation. In this step, the user interactively rotated each ROI to a vertical alignment to ensure consistency for downstream analysis.

Once all ROIs were oriented, a final series of adjustments and a critical masking step were performed for each replicate. The user was first allowed to make fine-tuned adjustments to

brightness, contrast, and flat-fielding specific to that ROI. Following this, the user manually traced a precise polygon around the gel boundary. The area within this polygon was used to generate a binary gel mask, ensuring that all subsequent analysis was confined to the gel region, effectively excluding the background.

To account for non-uniform background signal within the gel itself, an interactive baseline correction was performed. The vertical intensity profile of the masked gel was plotted, and the user selected points corresponding to the background signal. A baseline was then generated by linear or cubic interpolation of these points and subtracted from the image, producing a baseline-corrected intensity profile.

Next, curved interface analysis of hydrogel images was performed using a custom interactive Python workflow that enabled precise definition and quantitative characterization of gel-fluid boundaries and penetration regions. Users first selected the desired interface mode (horizontal interface or gel edges) and optionally enabled advanced visualizations or penetration area annotation. Images were preprocessed with percentile-based colormap enhancements to improve visibility of gel structures. For each replicate, a region of interest (ROI) could be selected, after which the user interactively traced the gel interface using a resizable, rotatable drawing tool. The resulting interface curves were automatically smoothed and interpolated to generate continuous profiles across the gel width. From these curves, the workflow computed intensity profiles along and perpendicular to the interface, as well as their first and second derivatives, to capture fine structural features. A parallel module allowed manual annotation of complex penetration areas using multi-polygon drawing tools, with all resulting masks and polygon coordinates stored for analysis. All interface and penetration data were scaled back to original image dimensions, converted to physically meaningful units, and stored alongside metrics such as mean interface position, penetration area, and standard deviations, enabling detailed, reproducible comparison across replicates.

Following curved interface annotation, quantitative morphometric analysis of the gel region was performed to extract detailed metrics of shape and size. For each replicate, the binary gel mask was used to compute total area in mm^2, as well as width and height profiles along orthogonal directions with propagation of pixel-level measurement errors. Profiles were derived by summing the mask along image rows and columns and converting to physical units using the known scale factor. The workflow generated summary metrics including total area with uncertainty, maximum and average widths and heights with associated errors, and visualizations showing the segmented gel region alongside width and height profiles with error bars. All calculated metrics, raw profiles, and generated plots were stored within the replicate data structure, ensuring traceable, reproducible comparison of gel geometry across all experimental conditions.

Following interface annotation, an advanced overlay analysis was conducted to quantify penetration and interface-related metrics within the gel region. The processed replicate images were analyzed by aligning the manually defined interface with the gel mask to extract tight bounding regions for visualization. Interactive widgets allowed users to adjust intensity scaling, median filtering, and thresholding parameters (including adaptive Gaussian or Otsu methods) to robustly segment particle regions above the interface. A zoomed region of interest, defined relative to the interface position, was analyzed to compute metrics such as particle count, area, maximum penetration depth (both Euclidean and vertical from interface), and average distances with associated standard deviations. This workflow also supported multiple manually defined penetration polygons per replicate, calculating region-specific particle metrics and summarizing total penetration area and intensity. All measurements were automatically converted to physical

units (mm or mm^2) using the known pixel size, and rich, interactive visualizations were generated to ensure consistent and reproducible interpretation across replicates.

Upon completion of the analysis for all replicates, the workflow automatically generated and saved a comprehensive set of results. For each replicate, a multi-sheet Microsoft Excel file was created containing a summary of all calculated metrics (e.g., gel area, width, height, particle counts, penetration statistics) and the raw data for all generated profiles. Concurrently, a series of high-resolution PNG figures were saved to a plots subdirectory, including images of the masked gel, width/height profiles, and detailed visualizations of the interface analysis, such as particle distribution and intensity relative to the interface. This entire data and figure generation process was managed using parallel processing to optimize performance and reduce total analysis time.

In addition to this image-based analysis, a separate Python workflow was developed to support the organization and aggregation of experimental metadata stored in Excel files. Quantitative aggregation of experimental Excel metrics was performed using a custom Python workflow that automates directory selection, metadata extraction, and data merging. The user selects a top-level folder via a graphical interface, after which the script recursively scans for Excel files containing "metrics" in their paths while excluding blanks or partial analyses. It extracts metadata—including cycle count, replicate number, concentration, and treatment time—from file and folder names using regular expressions to generate consistent, descriptive sheet labels. The workflow identifies all available worksheet types across the dataset and creates merged Excel workbooks for each type, saving them in an organized "merged_analyses" directory with subfolders for each sheet type. Within each merged file, data from all replicates is included on separate, clearly labeled sheets, enabling streamlined and reproducible analysis of large experimental datasets.

For quantitative comparison of penetration metrics across experimental conditions, data from the merged Excel files (each containing replicate-level summaries of penetration region area and particle count) were imported into Python for further analysis. Each replicate sheet was parsed to extract the "Penetration Region Area" and "Particle Count" values, with missing measurements explicitly treated as zero to ensure consistent inclusion of all replicates. For each duty cycle, the top three replicates (by penetration area) were selected, and a weighted average and standard deviation were calculated using particle count as weights to capture measurement precision. These weighted metrics for DBPC HMSN and MSN particles were then combined into a single dataframe and visualized as grouped bar charts, showing side-by-side comparisons of mean penetration region area across duty cycles with error bars indicating the weighted standard deviation.

FIGURES:

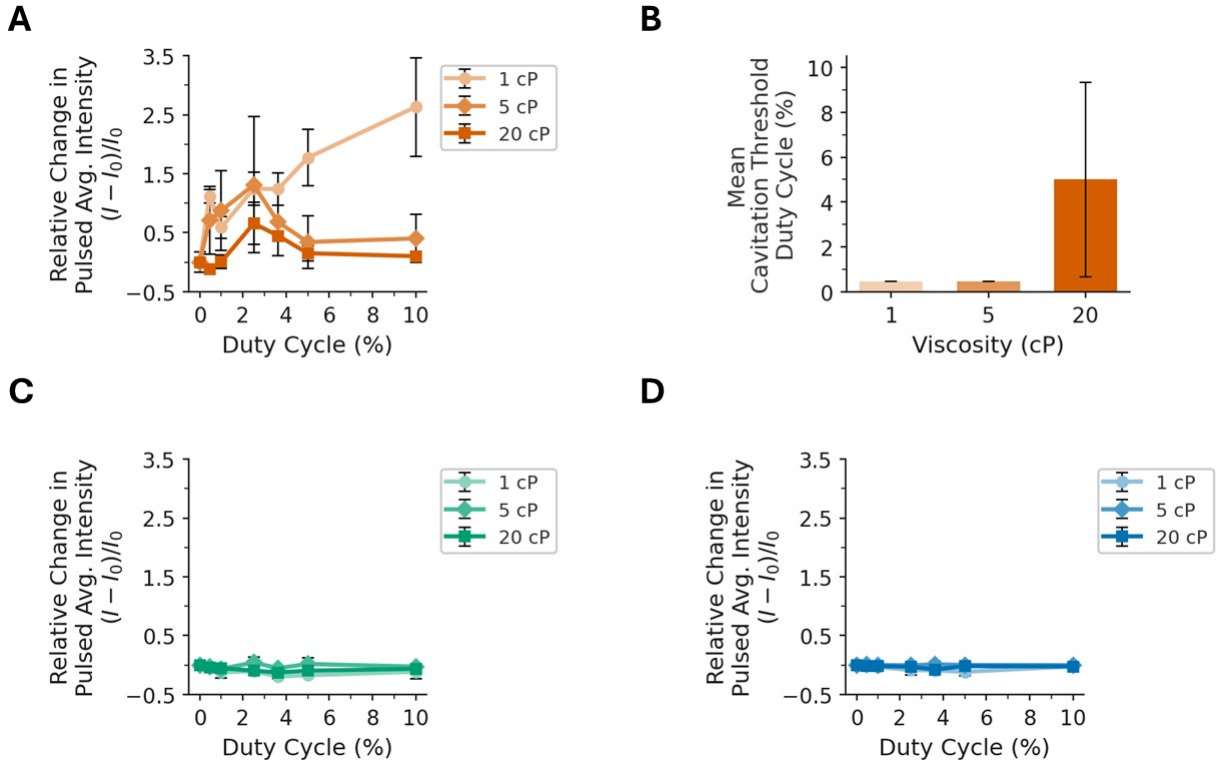

Figure S1. (A) Passive cavitation data for ultrapure water and PEG 2000 solutions with DBPC HMSNs at viscosities of 1, 5, and 20 cP. (B) Cavitation thresholds for solutions at 1, 5, and 20 cP viscosities. Passive cavitation data for (C) MSNs and (D) 1X PBS. n = 3 for all conditions. Error bars signify one standard deviation of the mean.

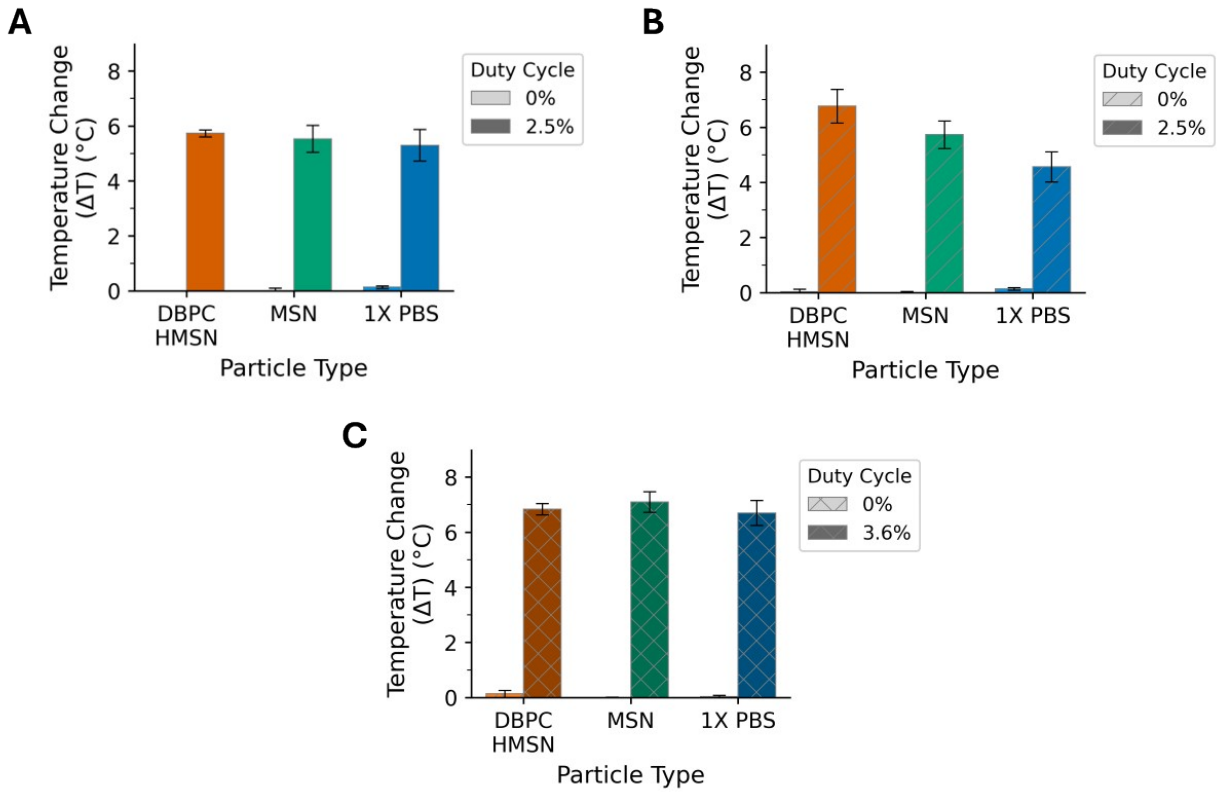

Figure S2. Temperature change before and after HIFU treatment (n = 3) for (A) 2% gelatin, (B) 4% gelatin, and (C) 8% gelatin. Error bars signify one standard deviation of mean.

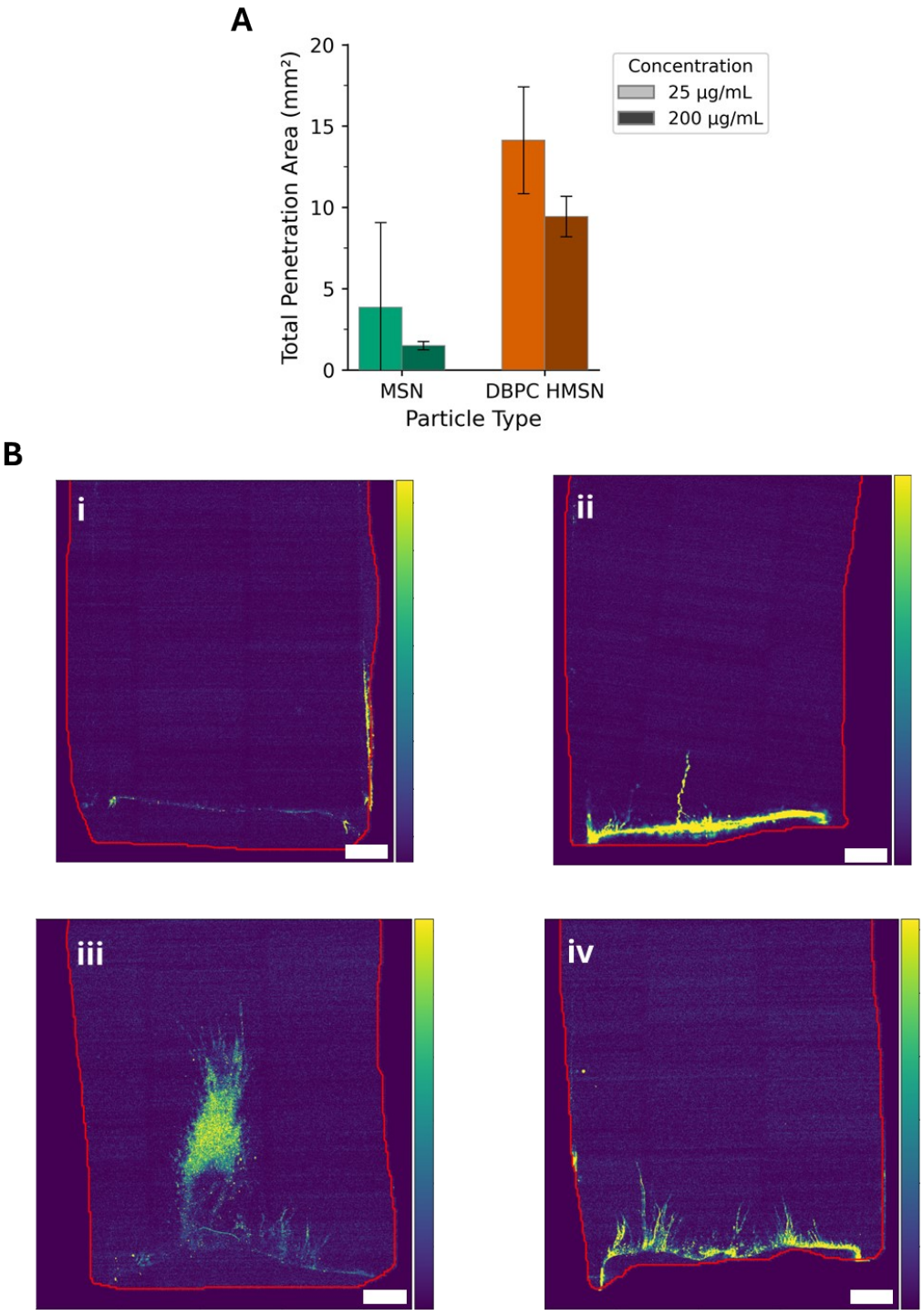

Figure S3. (A) Total penetration area (n=3) of MSNs and DBPC HMSNs driven into 2% gelatin at 2.5% duty cycle. Error bars signify one standard deviation of mean. Statistical significance between the no HIFU and HIFU groups was tested using an independent-samples t-test (*$p < 0.05$). (B) Rows = particle type (top: MSN; bottom: DBPC-HMSN); columns = concentration (left: 25 µg/mL; right: 200 µg/mL). Pseudocolor scale indicates fluorescence intensity, ranging from low (bottom of colorbar) to high (top). Scale bar = 1 mm.

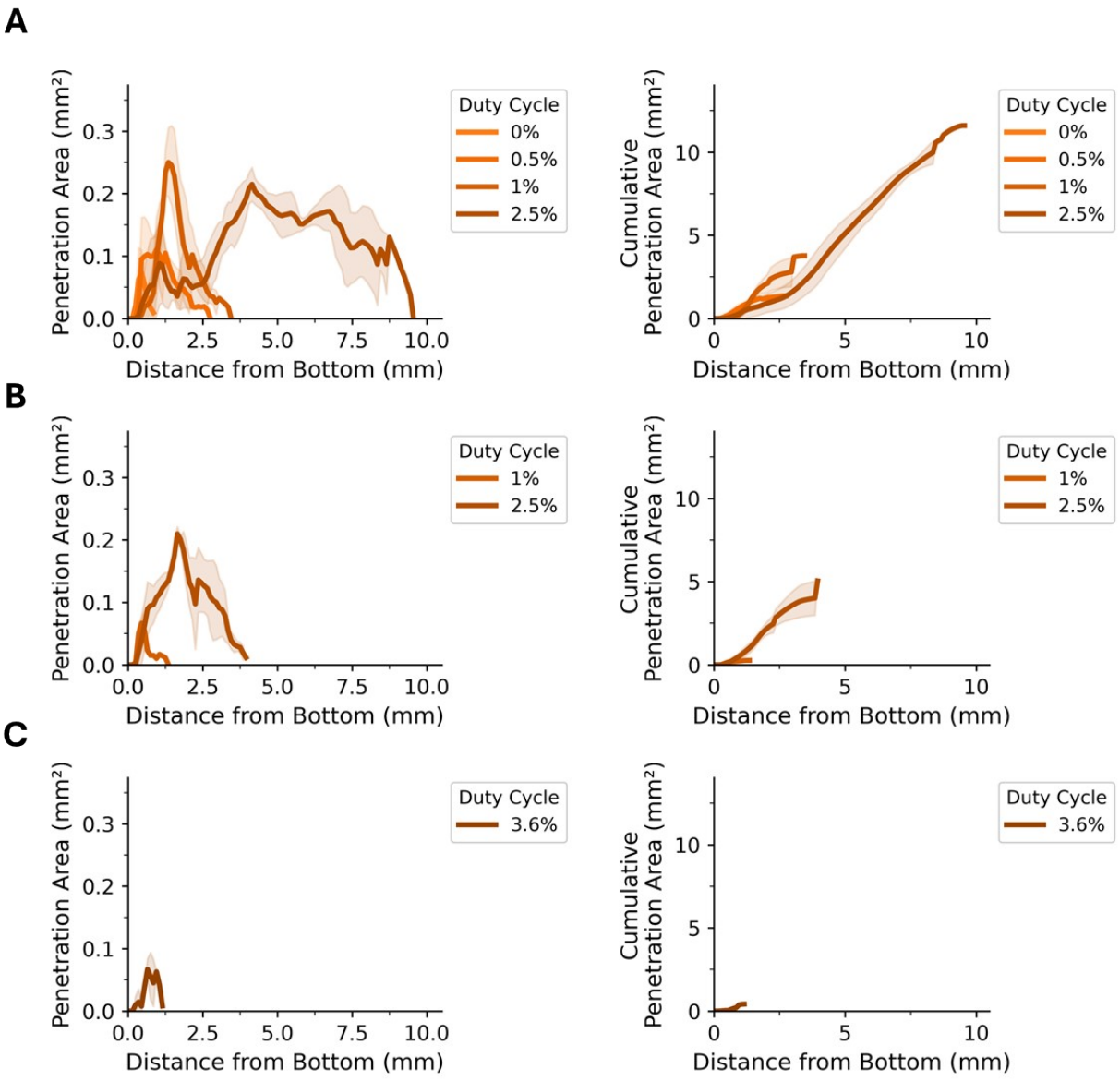

Figure S4. Penetration area (left) and cumulative penetration area (right) profiles of DBPC HMSNs in (A) 2% gelatin, (B) 4% gelatin, and (C) 8% gelatin. Data represent n = 3 replicates; shaded regions indicate one standard deviation of mean. Missing data correspond to absence of particle penetration.

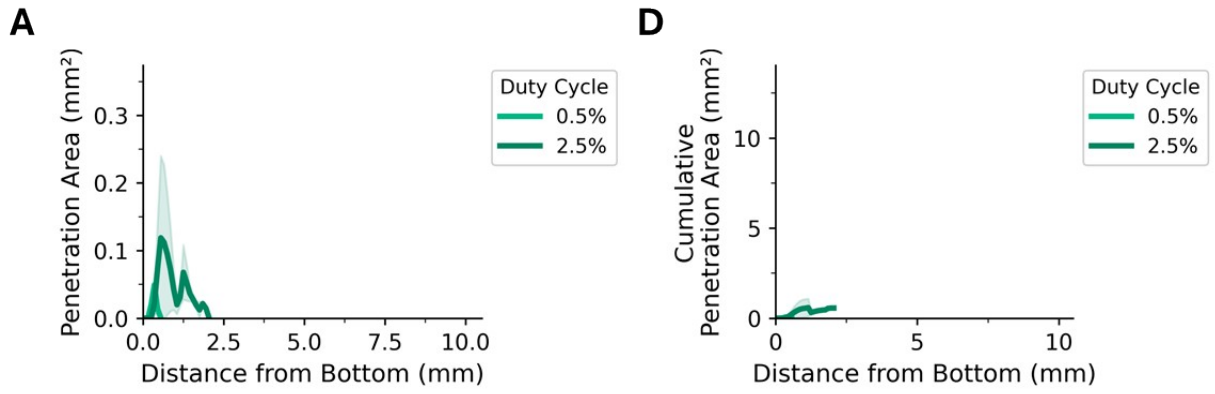

Figure S5. Penetration area (left) and cumulative penetration area (right) profiles of MSNs in (A) 2% gelatin. Data represent n = 3 replicates; shaded regions indicate one standard deviation of mean. Missing data correspond to absence of particle penetration.

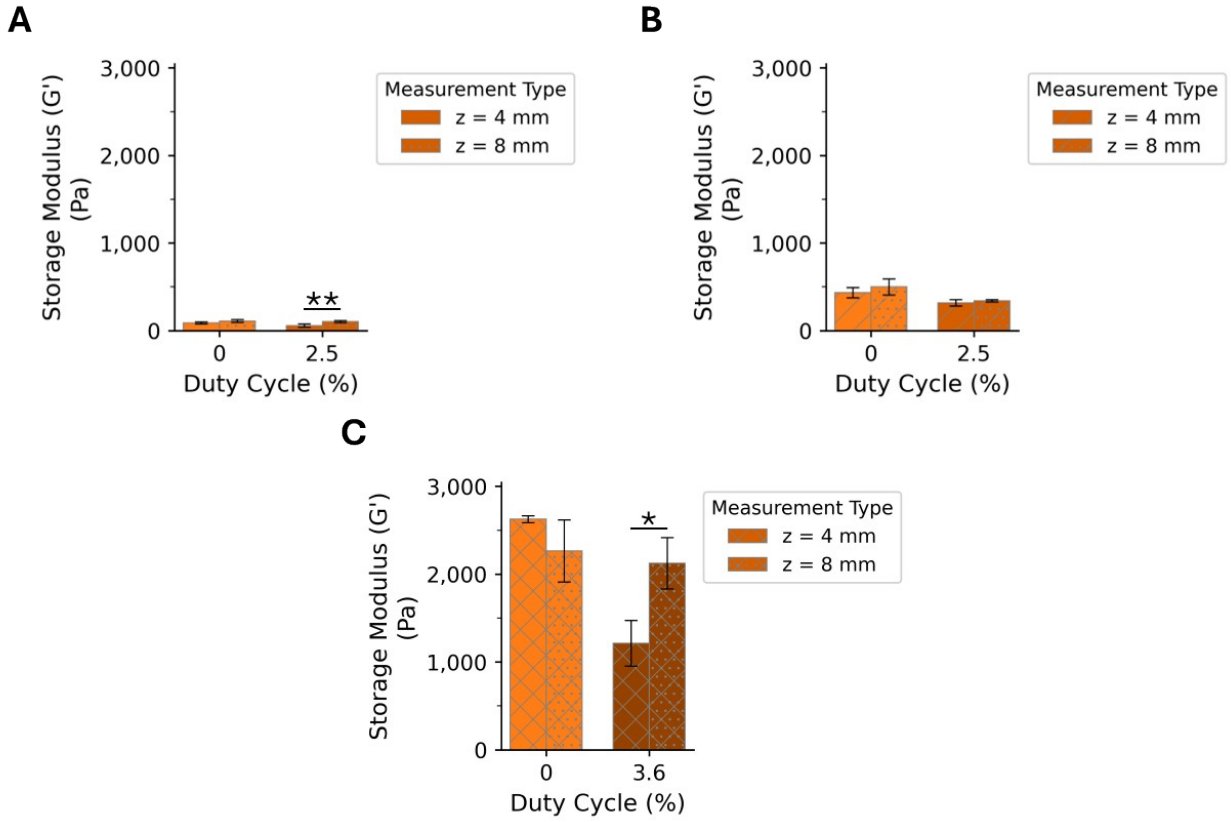

Figure S6. Storage modulus (G′) of (A) 2%, (B) 4%, and (C) 8% gelatin hydrogels before and after HIFU treatment with DBPC HMSNs. Each hydrogel was sectioned into two 4-mm layers: the bottom layer (0–4 mm) and the top layer (4–8 mm). At each duty cycle, the left bar represents the bottom layer and the right bar represents the top layer. Each section was analyzed separately by rheometry (n = 3). Error bars signify one standard deviation of mean. Statistical significance between bottom layer (0-4 mm height) and top layer (4-8 mm height) measurements was tested using a one-tailed paired-samples t-test (*$p < 0.05$, **$p < 0.01$).

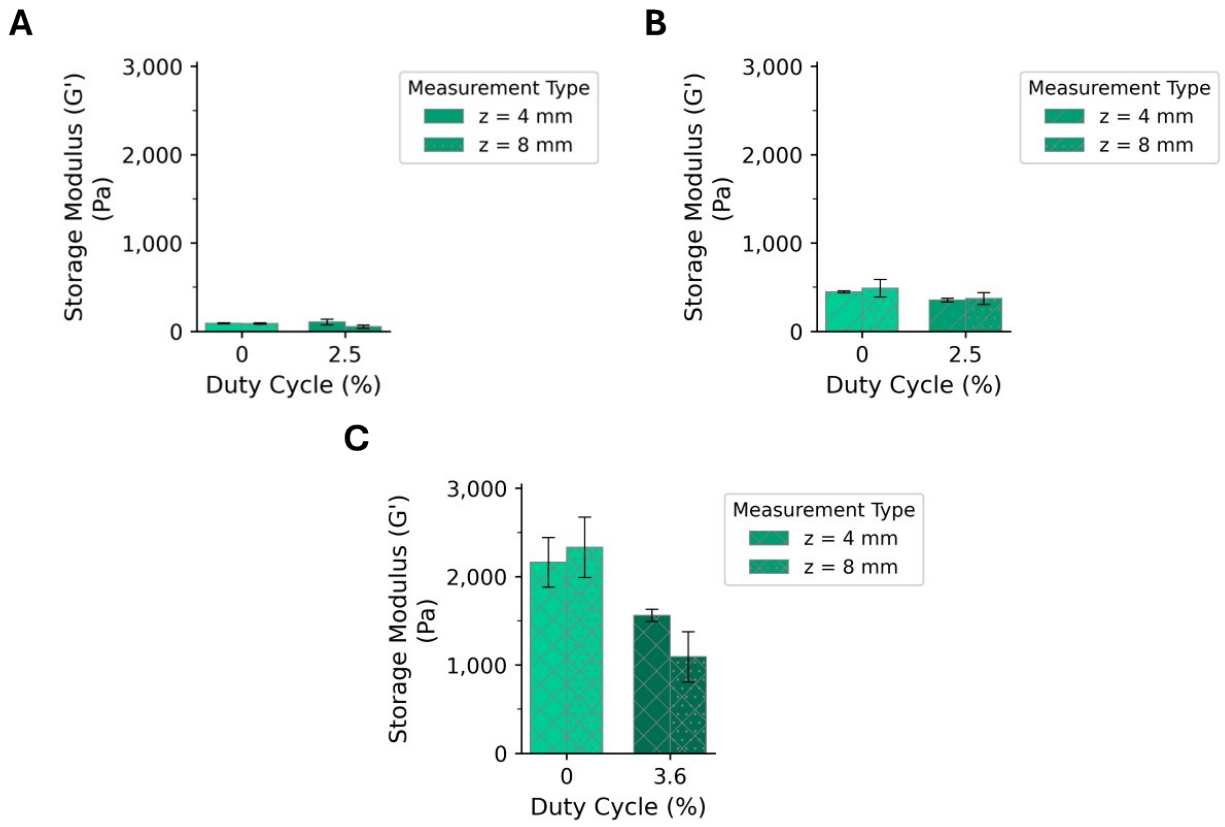

Figure S7. Storage modulus (G′) of (A) 2%, (B) 4%, and (C) 8% gelatin hydrogels before and after HIFU treatment with MSNs. Each hydrogel was sectioned into two 4-mm layers: the bottom layer (0–4 mm) and the top layer (4–8 mm). At each duty cycle, the left bar represents the bottom layer and the right bar represents the top layer. Each section was analyzed separately by rheometry (n = 3). Error bars signify one standard deviation of mean.

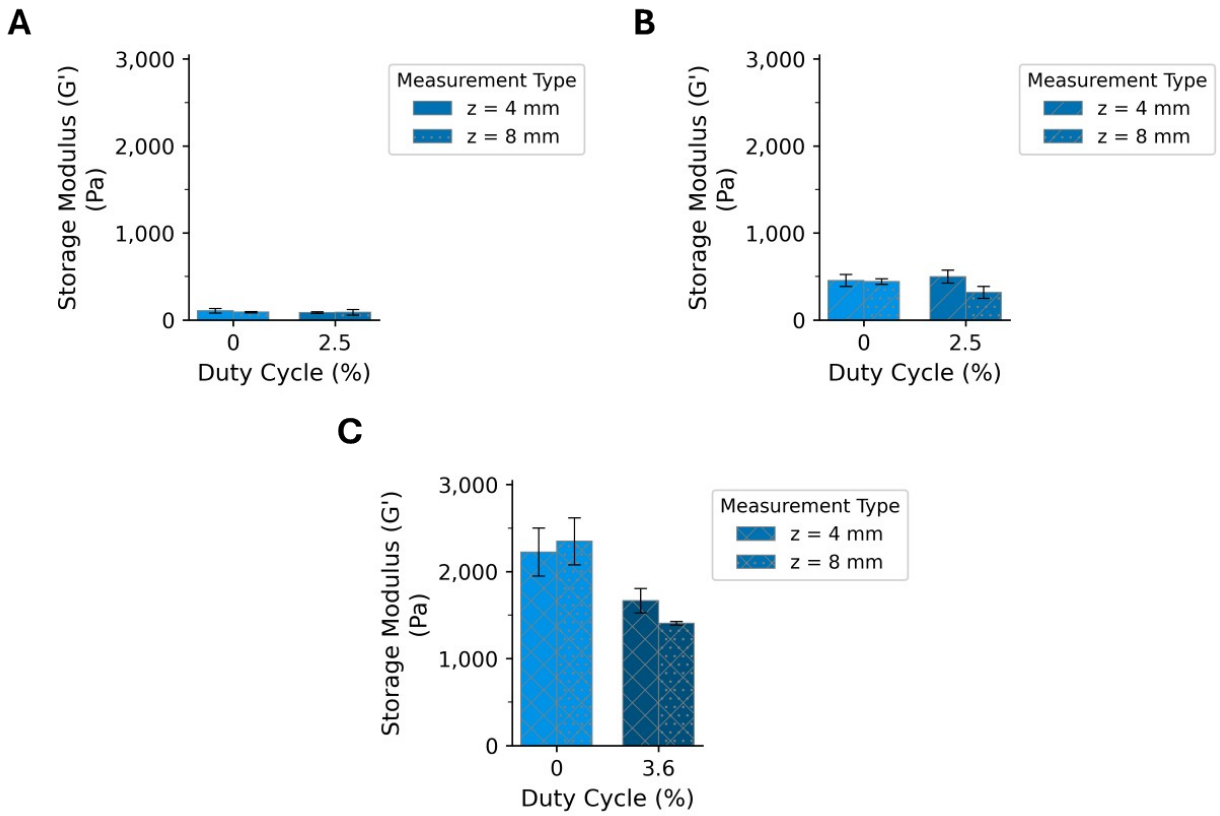

Figure S8. Storage modulus (G′) of (A) 2%, (B) 4%, and (C) 8% gelatin hydrogels before and after HIFU treatment with 1X PBS. Each hydrogel was sectioned into two 4-mm layers: the bottom layer (0–4 mm) and the top layer (4–8 mm). At each duty cycle, the left bar represents the bottom layer and the right bar represents the top layer. Each section was analyzed separately by rheometry (n = 3). Error bars signify one standard deviation of mean.

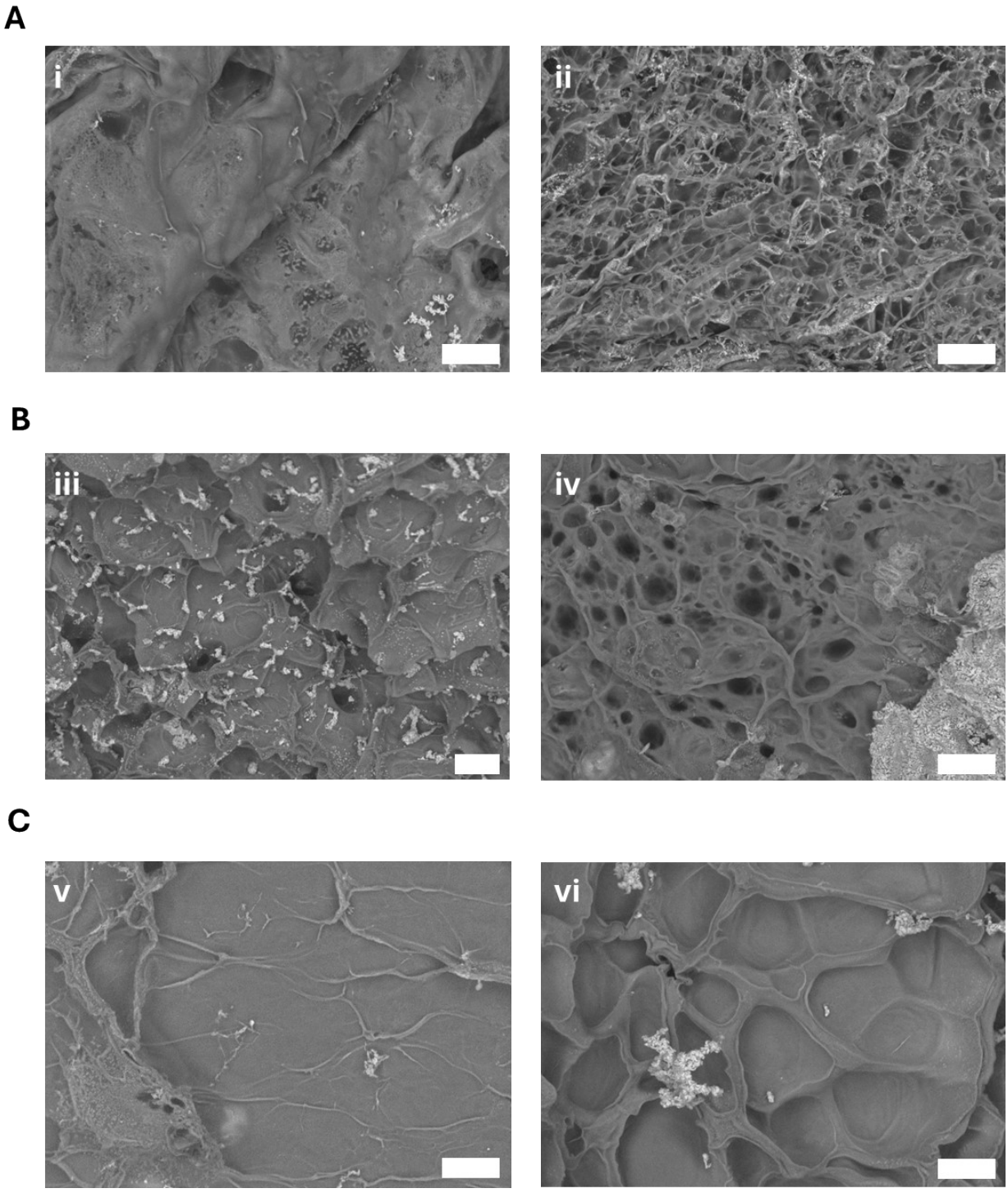

Figure S9. Scanning electron microscopy images of untreated (left panel: i, iii, & v) and treated (right panel: ii, iv, & vi) (A) 2% gelatin (2.5% duty cycle), (B) 4% gelatin (2.5% duty cycle), and (C) 8% gelatin treated (3.6% duty cycle) with MSNs. Scale bar = 20 μm.

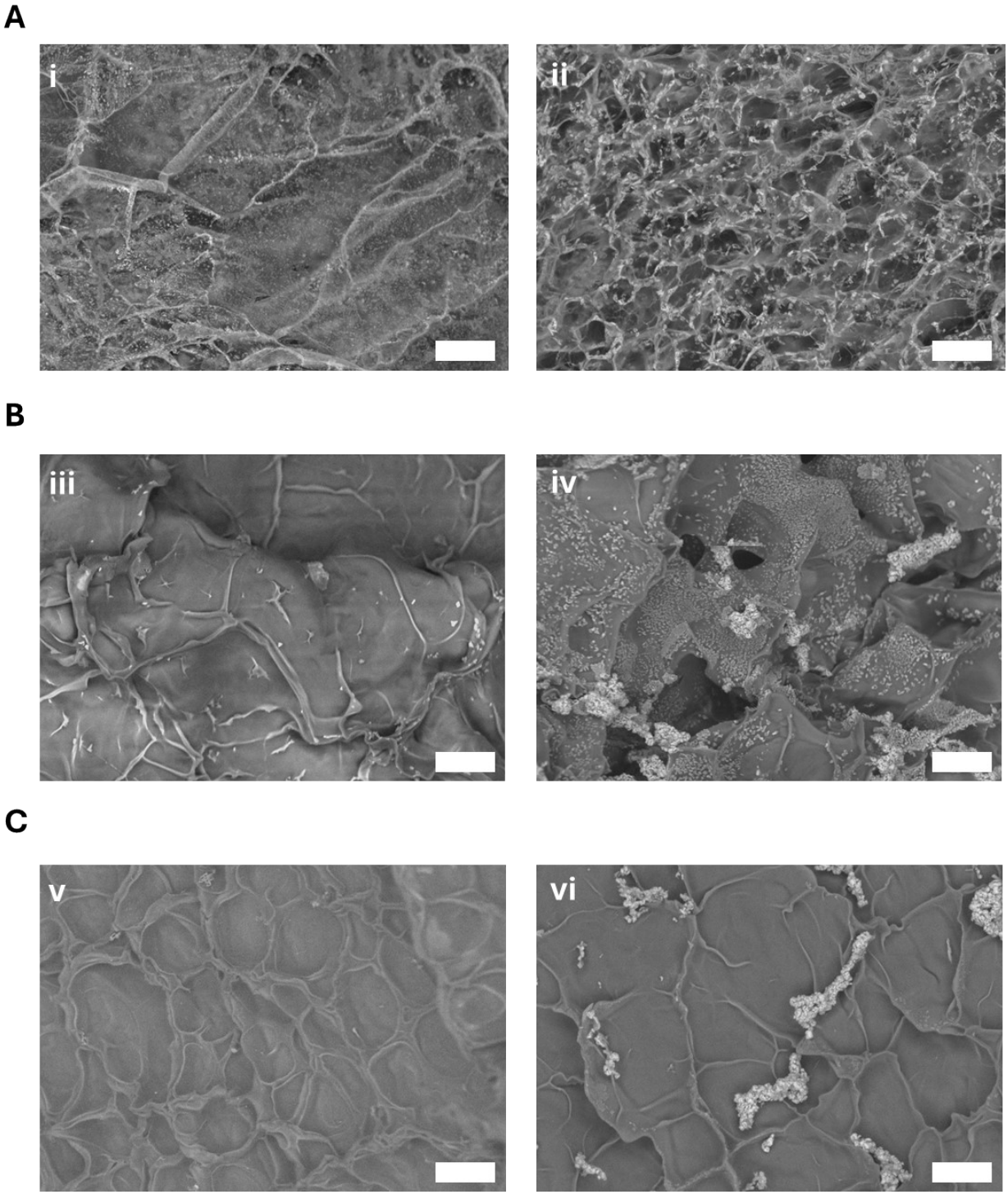

Figure S10. Scanning electron microscopy images of untreated (left panel: i, iii, & v) and treated (right panel: ii, iv, & vi) (A) 2% gelatin (2.5% duty cycle), (B) 4% gelatin (2.5% duty cycle), and (C) 8% gelatin treated (3.6% duty cycle) with 1X PBS (no particles). Scale bar = 20 μm.

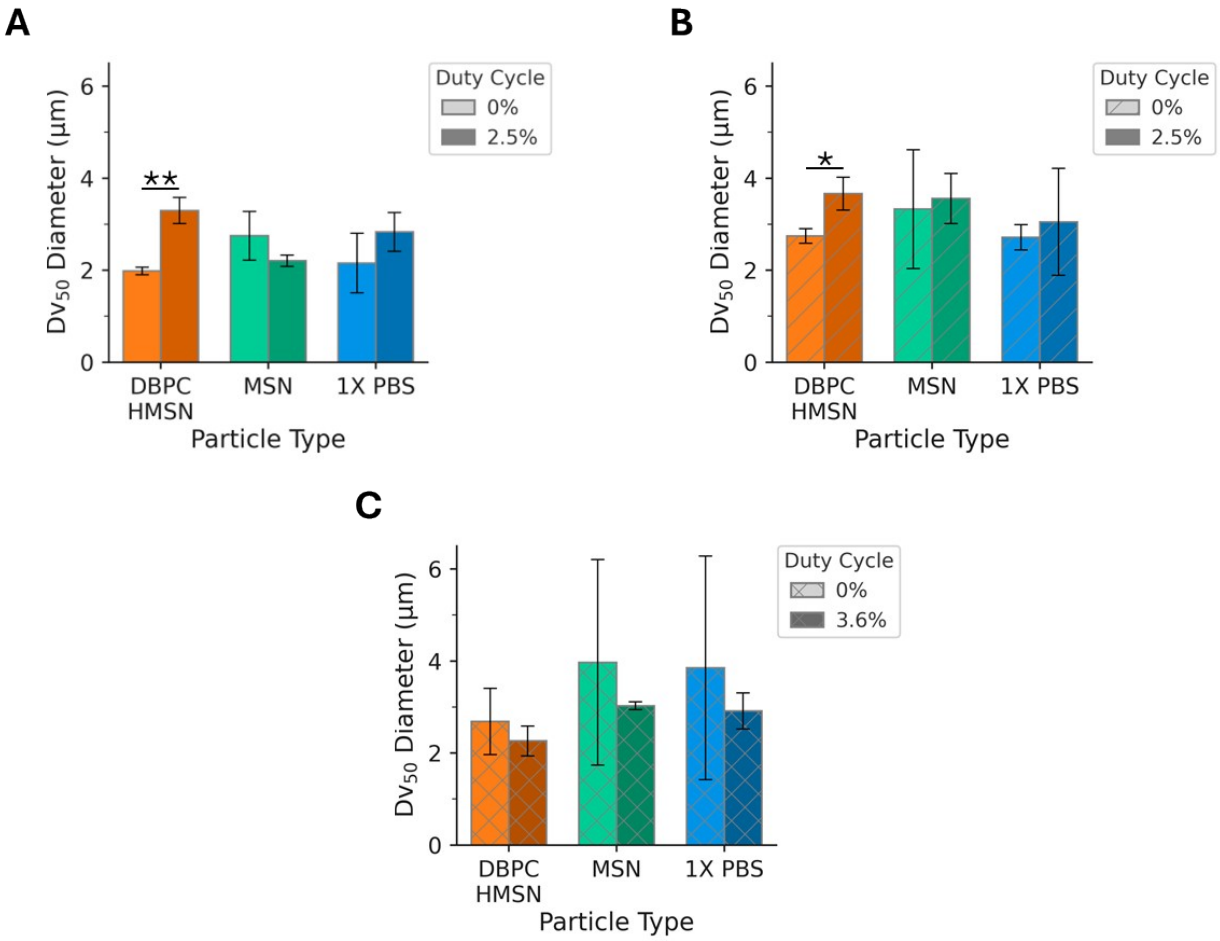

Figure S11. 50th percentile of volume-weighted diameter (n=3) of (A) 2% gelatin, (B) 4% gelatin, (C) 8% gelatin with and without HIFU. n=3. Error bars signify one standard deviation of mean. Statistical significance between the no HIFU and HIFU groups was tested using a one-tailed independent-samples Welch's t-test (*$p < 0.05$, **$p < 0.01$).

REFERENCES.

1 A. Yildirim, R. Chattaraj, N. T. Blum, D. Shi, K. Kumar and A. P. Goodwin, *Advanced healthcare materials*, 2017, **6**, 1700514.
2 T. B. Alina, S. A. Saemundsson, L. E. Mortensen, Y. Xu, J. W. Medlin, J. N. Cha and A. P. Goodwin, *Adv Funct Materials*, 2024, 2412344.
3 T. B. Alina, V. A. Nash and K. L. Spiller, *Front. Chem.*, DOI:10.3389/fchem.2020.593422.
4 T. Murugesan and M. Perumalsamy, *J. Chem. Eng. Data*, 2005, **50**, 1290–1293.
5 T. E. Oliphant, *Guide to numpy*, Trelgol Publishing USA, 2006, vol. 1.
6 T. B. Alina, H. B. Kirkpatrick, N. M. Bower, S. D. Curry, T. R. Ausec, S. A. Saemundsson, E. N. Mueller, C. W. I. Shields, J. N. Cha and A. P. Goodwin, *ACS Applied Nano Materials*, 2023, **6**, 13720–13729.
7 T. B. Alina, *Available online: https://github.com/ThundaNann/hydrogel_transport*.
8 T. B. Alina, *Available online: https://github.com/ThundaNann/Cavitation-signal-intensity.git*.
9 S. Sakai, University of Illinois, Urbana-Champaign, 2003.
10 W. M. B. M. Yunus and A. B. A. Rahman, *Appl. Opt.*, 1988, **27**, 3341.
11 M. Bailey, B. Gardner, M. Alunni-Cardinali, S. Caponi, D. Fioretto, N. Stone and F. Palombo, *Appl Spectrosc*, 2021, **75**, 574–580.